Computational and Theoretical Chemistry 1220 (2023) 113998

Contents lists available at ScienceDirect

Computational and Theoretical Chemistry

journal homepage: www.elsevier.com/locate/comptc

Transition metals incorporated on phosphorene sheet as cost-effective single atom catalysts for hydrogen evolution reaction: A DFT study

Sonia Iqbal [a,1], Khursheed Ahmed [b,1], Khurshid Ayub [c], Muhammad Hamid Butt [a], Ahmad Nauman Shah Saqib [b], Ahmed Lakhani [d], Ch. Muhammad Fahim Ayaz [e], Muhammad Ali Hashmi [b,*]

[a] Department of Chemistry, University of Management and Technology, C-II, Johar Town Lahore 54770, Pakistan
[b] Department of Chemistry, Division of Science & Technology, University of Education, 54770 Lahore, Pakistan
[c] Department of Chemistry, COMSATS University Islamabad, Abbottabad Campus, Abbottabad 22060, Pakistan
[d] Department of Biomedical and Health Sciences, Calumet College of St. Joseph, 2400, New York Ave, Whiting, IN 46394, United States
[e] Department of Chemistry, University of Agriculture, Faisalabad, Pakistan

A B S T R A C T

Hydrogen is an efficient alternative for conventional energy sources with a high gravimetric caloric value and zero-emission rate. Hydrogen evolution reaction (HER) is an efficient technique for hydrogen production via water electrolysis, but the process yields limited production of hydrogen gas due to less intrinsic activity of the electrode. Pt, in this case, is known as a state-of-the-art electrocatalyst for HER reaction, however, its application is limited due to high cost and less availability. In this study, the performance of less expensive transition metals embedded on phosphorene (TM@P) has been theoretically evaluated for HER through single-atom catalysis. TM@P sheet is optimized at various spin states. Gibbs free-energy change (ΔG_{H^*}) is calculated for the system with the most stable spin states to analyze the hydrogen binding strength on the surface of the catalyst, which is a key parameter to evaluate HER activity. The results showed that low-cost TM@P could be an effective alternative to noble metals with improved catalytic activity for HER, which is also supported by NBO analysis.

1. Introduction

More than 80 % of the world's energy requirement is driven by fossil fuels. However, the chemical combustion of fossil fuels generates various chemical substances that contribute the enormous environmental issues [1]. Major by-products of fossil fuel consumption that deteriorate the environment include CO_x, NO_x, and SO_x, which results in the production of classical/London smog, photochemical smog, acid rain, and also contribute to global warming. Moreover, the expanding monetary values due to non-homogeneous geological distribution and inaccessibility to the underground reserves make it harder to pursue conventional fuel [2]. Therefore, it is a global need to switch to greener, eco-friendly, and renewable energy sources.

Hydrogen fuel has recently gained much interest as it is environment-friendly with almost zero-emission and exhibits immense energy storage with a gravimetric caloric value of ~ 120 MJ kg^{-1} much higher as compared to other conventional fuels (petroleum; 45 MJ/kg, Coal; 24 MJ/kg, Natural gas; 34–38 MJ/m^3)[1,3–6]. Despite its abundance in nature, it's obscure to isolate pure hydrogen. Currently, over 95 % of hydrogen production is based on fossil fuel reforming, which results in extensive CO_2 emissions [1,7,8]. Among currently practiced technologies, only water electrolysis is promised to be the greener source to obtain a large amount of hydrogen, however, it contributes to only 4 % of hydrogen production worldwide (Scheme 1b) [1,9,10]. Water electrolysis is comprised of two semi-reactions; hydrogen evolution reaction (HER) and oxygen evolution reaction (OER) taking place at cathode and anode, respectively. HER is one of the safer and nature-friendly ways to produce hydrogen by water electrolysis, [11] and probably the most studied reaction in electrochemistry since its discovery [12]. Thermodynamically, HER is a multi-step reaction, proceeds either through Volmer-Heyrovsky or Volmer-Tafel steps on cathode interface in an electrolytic cell [13–15].

$$H_3O^+ + e^- + * \rightarrow H^* + H_2O \text{ (Volmer-step)}$$

$$H^* + H_3O^+ + e^- \rightarrow H_2 + H_2O \text{ (Heyrovsky-step)}$$

$$H^* + H^* \rightarrow H_2 \text{ (Tafel-step)}$$

The decisive step in the HER mainly depends upon the concentration

* Corresponding author.
E-mail address: muhammad.hashmi@ue.edu.pk (M.A. Hashmi).
[1] These authors have equal contribution.

https://doi.org/10.1016/j.comptc.2022.113998
Received 18 October 2022; Received in revised form 11 December 2022; Accepted 21 December 2022
Available online 24 December 2022

of H* (θ_H) [16,17]. A lower H* coverage ratio results in the Heyrovsky reaction, which proceeds by the combination of adsorbed hydrogen with a proton/water while attaining an electron from the surrounding. In the Tafel step, two neighboring H* combine to produce an H_2 molecule.

In recent years, substantial work has been done to investigate transition metal-doped phosphides (TMPs) as HER electrocatalysts, and the results reveal the activity equivalent to noble metals [1]. It has been reported that the electrocatalytic activity of the catalyst is directly proportional to the number of exposed active sites. However, the net activity of the electrocatalyst suffers a loss during electrochemical application due to their particle morphologies. It has been well established that the particle with smaller grain sizes are electrochemically more active than the larger ones because of the fact that they have more exposed metal atoms. In this regard, only a single atom-based catalysts (SAC) and double atoms-based catalysts (DAC), are receiving a great attention due to their extra ordinary electrocatalytic activity, statbility, and selectivity.[25,26] The SAC is observed to have a great effect on the electronic structure of the substrate, which ultimately results in the better efficiency and charge transport for optimal adsorption of the reactants.[27] Tiwari et al. fabricated and studied Pt-based catalyst with ultra low Pt loading of 1.4 μg supported on cm^2 area of graphitic tube deposited with Cu on inner walls and encapsulated in FeCo alloy. This volume of Pt loading is about 1/80th of the commercial Pt loading on graphene sheets. The authors observed that the newly fabricated electrocatalyst performs 96 times better than Pt/C, and achieved 10 mA cm^{-2} at overpotential of only 18 mV.[28] Nevertheless, Cu and Ru supported on *N*-doped graphene also exhibit an overpotential of 8 mV to deliver 10 mA cm^{-2}.[29] A very recent DFT study on MoS_2 is carried out to modify and enhance their functionality by adsorption of various single transition metals. Wang et al. reported that SAC-based Co@MoS_2 is proven activity as a bifunctional electrocatalyst for water splitting with an ultralow overpotential of 0.3 V.[30] A first-principle-based calculation revealed that TMN_x-doped (where TM = Ti to Ni) graphene SACs also exhibit excellent electrocatalytic activity for nitrate reduction reaction (eNO_3RR), which consent with experimental results. [31] As an extension of SAC, Wu et al. presented a theoretical perspective of DAC, anchored on a suitable substrate as metal dimers. DACs are observed with comparatively better electrocatalysis activity due to multiple binding sites, mutual synergistic effect, and enhanced electronic properties.[32] Ha et al. used machine learning-based approach to theoretically study the 3d-5d TM-based SACs embedded in N_xC_y moieties, and predicted that TM@N_2C_2 complexes tends to form more easily, with higher electrochemical activity and chemical stability. Moreover, they reported some complexes with efficient bifunctionality. The higher stability are correlated with the stronger chemical bond between metal atom and support, which tends to resist the aggregation and dissolution of the metal atoms.[33] The major hurdle to HER is the lesser availability of efficient and cost-effective electrode material with high intrinsic activity. Pt is considered as the state-of-the-art electrocatalyst with excellent HER activity and long-term stability in acidic media, however, its application at industrial scale is limited due to its scarcity and less availability [44–46]. Therefore, in the last few decades, researchers have been searching to develop relatively cheap and highly efficient HER electrocatalysts. Fortunately, some of the heteroatomic-doped transition metals showed comparable activity to standardized Pt-based catalysts [34,47–52]. However, the major issue in their practical application arises due to their less stability, limited on-edge active sites, and susceptibility to corrode under acidic media [53,54].

Recently, phosphorus-based transition metals gained a lot of attention as efficient electrocatalysts due to their high intrinsic activity and low cost [1]. Their wide-scale applications in various fields, such as hydroprocessing [18], hydrodenitrification [19], and hydrodesulfurization [20] (HDS), demonstrate their efficient catalytic activities. Moreover, their role in photocatalytic hydrogen production [21,22] and electrochemical oxygen production [23,24] has also been demonstrated due to their high electrical conductivity and tunable electronic structure. Phosphorene, which is an artificially created nanostructured black phosphorous (BP), is predicted to be a potential electrocatalyst for HER [55–57]. Recent studies on phosphorene nanoparticles demonstrated excellent catalytic activity for HER in acidic media [58]. Liu and Rodriguez performed computational calculations on Ni_2P using density functional theory (DFT) and evaluated its highly improved HER activity, even superior to Pt-based catalysts [34]. Xu et al. predicted the efficient activity of nanoporous phosphide-based Fe nanosheets [35], and plenty of work has also been done in the recent era on various P-based TMs, such as CoP [36] WP, [37,38] MoP, [39,40] Cu_3P, [41,42] etc. to prove their elevated HER activity. He et al. examined MoS_2 flakes on phosphorene nanosheets, and claim the better HER activity of this electrocatalyst [59]. Shao et al. reported experimental work on phosphorene to functionalize with NH_2 and observed that the catalyst has an enhanced catalytic activity for HER [57]. Experimentally, the electrocatalytic activity of 2D BP-based materials is being observed to have an inverse relation with the number of layers in the 2D nanostructures, i.e., decreasing the size of the nanostructure can enhance the catalytic activity of the material towards HER [60]. There are a number of experimental reports on the production of hydrogen and water splitting using similar materials.[61–64] In this computational approach, we have discussed the effect of adsorption of first transition series elements (viz Sc, Ti, V, Cr, Mn, Fe, Co, Ni, Cu, and Zn) on the catalytic performance of pure phosphorene for HER, using density functional theory (DFT) calculations. We evaluated the catalytic performance of various metallic-adsorbed BP by computing their theoretical free energy (ΔG_H) values for hydrogen adsorption For the catalyst, to have an extraordinary HER catalytic performance, the ΔG_H value for hydrogen adsorption must be zero, which indicates the moderate hydrogen binding strength to the catalyst surface [65].

2. Computational details

All DFT calculations in this study were performed with hybrid functional of Perdew, Burke, and Ernzerhof (PBE0) [66,67] on Gaussian09 (Rev. D01) [68], and the models have been visualized using GaussView 5.0 (Gaussian Inc.) and CYLview. The TM@P sheets have been optimized followed by the frequency calculations to calculate free-energy (using equation (1)) using Ahlrich's triple-zeta (ζ) basis set def2-TZVP [69] along with Grimme's empirical D3 correction [70,71]

$$\Delta G_{H^*} = \Delta E_{H^*} - T\Delta S_H + \Delta E_{ZPE} \quad (1)$$

where ΔE_H is hydrogen adsorption energy, ΔE_{ZPE} is the zero-point energy change for adsorbed hydrogen and gaseous phase hydrogen, T denotes temperature (T = 298.15 K), and ΔS_H is entropy difference. At 298.15 K, $T\Delta S_H$ doesn't change and equals −0.20 eV. The hydrogen adsorption energy (ΔE_{H^*}) is defined as

$$\Delta E_{H^*} = E_{(TM@P+H)} - E_{(TM@P)} - \frac{1}{2}E_{H_2} \quad (2)$$

where $E_{(TM@P+H)}$ and $E_{(TM@P)}$ are the energies of the complex with and without adsorbed hydrogen, respectively, and E_{H_2} is the total energy of the gaseous phase hydrogen molecule. Zero-point energy (ΔE_{ZPE}) is obtained as:

$$\Delta E_{ZPE} = E_{ZPE^{H^*}} - E_{ZPE^*} - \frac{1}{2}E_{ZPE^{H_2}} \quad (3)$$

where $E_{ZPE^{H^*}}$ represents the zero-point energy for adsorbed hydrogen on TM@P, E_{ZPE^*} represents the zero-point energy for an active site, i.e., phosphorene-based TM only, and $E_{ZPE^{H_2}}$ is the zero-point energy of H_2 in the gas phase [45]. Infiite sized 2D systems using periodic boundary condition have been used for the calculation of HER activity through DFT calculations in the past.[50,52].

All the results are analyzed and compared based on the Sabatier principle, which states that the efficient catalytic activity may be

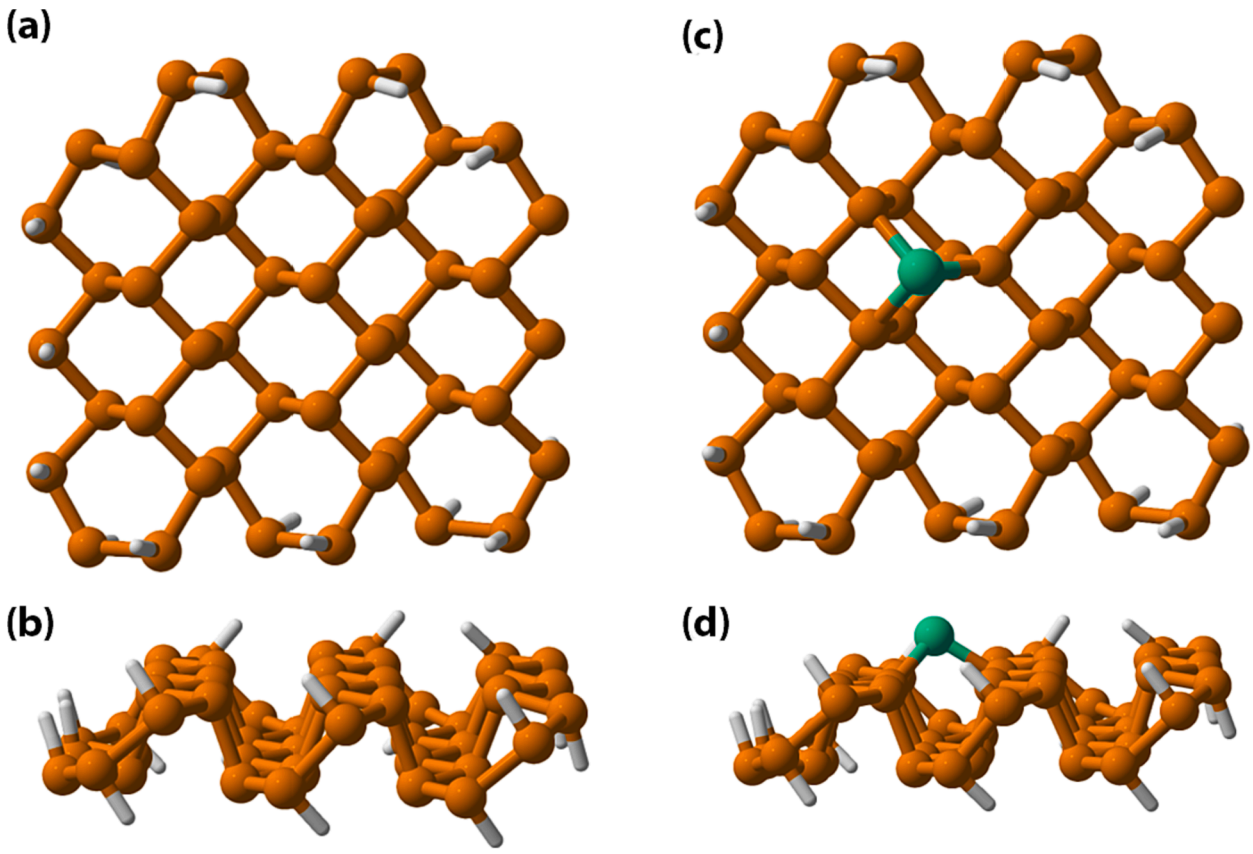

Fig. 1. Depiction of two-dimensional, single-layered, optimized phosphorene sheet. H atoms have been added to complete the valence; (a) and (b) show the top and side view of optimized phosphorene sheet, respectively while (c) and (d) show the top and side view of optimized Cu@phosphorene complex. Cu atom is shown in green color. (For interpretation of the references to color in this figure legend, the reader is referred to the web version of this article.)

observed for the electrocatalysts with intermediate free-energy change (or surface adsorption energy) i.e., $\Delta G_{H^*} \approx 0$ [72]. More negative ΔG_{H^*} value represents the stronger adsorption of the H atom on the catalytic surface, thus leading to low reaction kinetics and poisoned catalyst by binding permanently, while the catalyst with positive ΔG_{H^*} value results in weak interaction with adsorbed H atom, hence desorption occurs before activation. Thus, for an efficient HER electrocatalyst, free-energy change must be closer to zero, which creates optimal conditions for adsorption and desorption of the H atom [60]. There have been a number of reports with DFT-based calculations and Sabatier principle to efficiently analyze and evaluate the catalytic activity of various materials for HER [73–79].

3. Results and discussion

3.1. Surface geometry and stability

The binding geometries and adsorption energies have been calculated for transition metals from the first transition series (Sc to Zn) adsorbed on the phosphorene sheet, and their catalytic properties have been described using the results from DFT calculations. The adsorption of atomic hydrogen on these SACs has also been investigated and their recombination into the H_2 molecule has been proposed based on the Gibbs free energies of the SACs under study. During adsorption, metal atom sits on top of the cavity instead of fitting in the center of the cavity. We already reported it during our previous study using Cu@P fro CO oxidation reaction.[80] Similary in the current study different positions have been calculated for adsorption and the representative figure and table for the most stable system (Ti@P) has been given at Table S2 and Figure S1.

Phosphorene is an artificially made two-dimensional zigzag-shaped semiconductor with puckered honeycomb-like structure and improved mechanical and electronic properties with a direct bandgap of 1 eV [81]. Phosphorene, also known as black phosphorous (BP), is comprised of Phosphorus atoms each bonded to three other phosphorous atoms in a single layer [43]. In order to efficiently evaluate HER catalytic activity of various TM@P sheets, a small section of infinite single-layered optimized BP is used as a prototype with a P—P bond length of 2.20 Å (Fig. 1). TM atom is adsorbed directly to phosphorus atoms in pure phosphorene sheet. The stability of the TM@P sheet is calculated to estimate whether it can be synthesized thermodynamically, by their binding energies (E_{bind}) using following equation [82]

$$E_{form[83]} = E_{TM@P} - (E_{TM} + E_P)$$

where $E_{TM@P}$ represents electronic energy of TM@P sheet, while E_{TM} is the energy of a single TM atom acting as SAC and E_P is electronic energy of optimized phosphorene sheet. For TM@P, we observed that more negative interaction energies exhibit greater affinity of SAC to phosphorene sheet over bulk metal, and the positive energies would result in the aggregation of metals on the surface of the substrate [82]. Our results shows that all the values for E_{int} lies between − 100 to − 300 kcal/mol representing that the formation of complexes is thermodynamically favorable and do not tend to aggregate into bulk material.[84] However, this might not always be the case as some previous studies elaborated that the TM,if bind chemically to the sheet, could be trapped kinetically into their adsorption site, and their energy barrier would be so high to overcome normally.[85–87] For instance, the formation enegy of g-C_3N_4 supported Pt and Pd SACs is calculated to be −2.95 eV and −2.17 eV, and later synthesized experimentally.[88] Moreover, in our previous studies, we have evaluated the stability of the TM at different adsorption sites and notice no considerable difference.[80].

Table 1
Stable spin states of corresponding TMs of the first transition series adsorbed on the surface of phosphorene.

Complex	Stable Spin State	Interaction Energies (eV)
Phosphorene-Sc	Doublet	−5.409
Phosphorene-Ti	Triplet	−8.006
Phosphorene-V	Quartet	−8.313
Phosphorene-Cr	Quintet	−11.780
Phosphorene-Mn	Sextet	−9.758
Phosphorene-Fe	Triplet	−11.087
Phosphorene-Co	Doublet	−9.031
Phosphorene-Ni	Singlet	−11.569
Phosphorene-Cu	Doublet	−8.838
Phosphorene-Zn	Singlet	−7.366

All of the complexes with and without TM atom are optimized at various spin states, and the most stable spin state with lowest energy (see Table 1) is used for further analysis.

3.2. NBO analysis and charge transfer

During the HER activity, rapid charge transfer caused by the excellent electrical conductivity of transition metals plays an important role [1]. Natural bonding orbitals (NBO) charge analysis of TM@P revealed that metals with explicit donor character perform better than others [89]. For instance, Ti@phosphorene ($\Delta G_{H^*} = -0.296$ eV) acts as a donor (with 0.988e charge), and transfers its charge density to phosphorene sheet. The resulting electron density on Ti (0.571e) is suitable for optimum hydrogen binding. The binding of the H atom on a metal atom can cause charge redistribution through charge transfer. This trend is similar for other metals as if we compare Ti result with Ni@phosphorene ($\Delta G_{H^*} = 0.954$ eV). NBO analysis, in this case, reveals that Ni acts as an acceptor and accumulates charge on its surface (−0.171e) from very surrounding P-atoms at the initial stage. After adsorption of a hydrogen atom on Ni@phosphorene, more charge is transferred by phosphorene sheet to Ni (−0.341e) and the hydrogen atom (−0.225e). Hence, the accumulation of more negative electron density at both atoms (i.e., Ni and H) makes it slightly difficult to develop an optimum compared to the Ti@phosphorene complex (Fig. 2).

3.3. Hydrogen binding and the spin states

The next step was to evaluate the HER efficiency of the electrocatalysts under study. The hydrogen binding strength is the key parameter to analyze HER catalytic activity for any material, which should neither be too weak nor too strong for an efficient electrocatalyst. [90] In case of weak hydrogen-catalyst interaction, there will be no reaction on the catalytic surface because it makes it difficult for the catalyst surface to bind the reactants, while stronger interactions make it harder for H_2 molecules to get desorbed from the catalyst surface, which also lowers the activity. It means that the catalysts with $\Delta G_{H^*} \approx 0$ are the best ones for HER.

Afterward, the adsorption of atomic hydrogen on the TM@P with the most stable spin state has been computed and ΔG_{H^*} for the complex has been calculated. The spin state of the complex changed after the addition of the hydrogen on the TM due to the addition of an extra electron of hydrogen atom. The ΔG_{H^*} values have been given in Table 2.

Free energies given in Table 2 provide a quite useful way for predicting the intrinsic activity of a catalyst under investigation for HER using DFT calculations. Yu Gan et al. reported poor adsorption intensity of hydrogen atom on pristine phosphorene sheet with ΔG_{H^*} value of 1.23 eV [60]. The accepted standardized criterion for the adsorption of intermediate is that the value of ΔG_{H^*} must be closer to thermal neutral/zero for effective HER performance. These descriptors can also predict the real active sites besides predicting the intrinsic activity of the HER catalyst. According to our results, Cost-efficient Ti-embedded

Table 2
Calculated free energy for an adsorbed hydrogen atom on the corresponding TM@P in their stable spin states.

Complex	Stable Spin State	ΔG_{H^*} (eV)
Phosphorene-Sc-H*	Triplet	15.89238
Phosphorene-Ti-H*	Doublet	−0.296
Phosphorene-V-H*	Triplet	−7.436
Phosphorene-Cr-H*	Sextet	−6.241
Phosphorene-Mn-H*	Sextet	−6.241
Phosphorene-Fe-H*	Quartet	−6.867
Phosphorene-Co-H*	Triplet	−7.452
Phosphorene-Ni-H*	Doublet	0.954
Phosphorene-Cu-H*	Singlet	−0.478
Phosphorene-Zn-H*	Doublet	−5.457

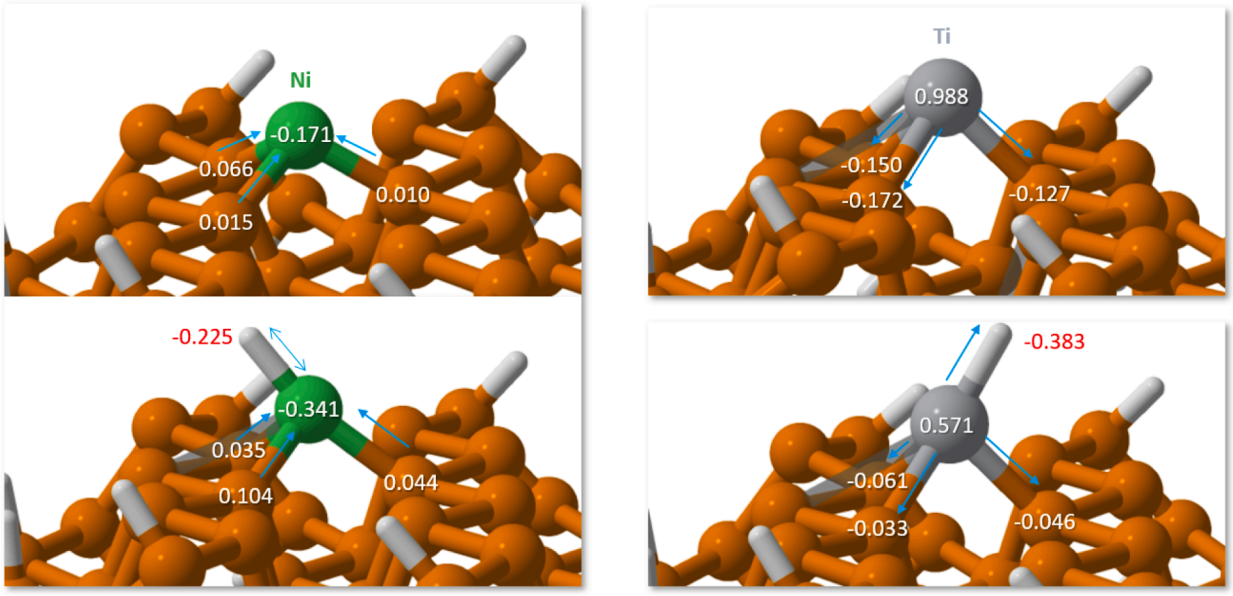

Fig. 2. Charge transfer analysis of H-adsorbed at Ni@phosphorene (left) Ti@phosphorene (right); Ni acts as an acceptor in the complex while Ti act as a donor.

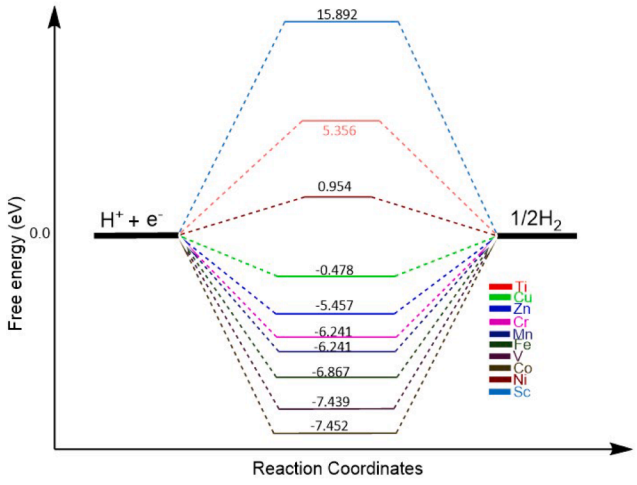

Fig. 3. Calculated free energy diagram for hydrogen evolution reaction of corresponding transition metals used as a single atom catalyst adsorbed on the phosphorene sheet. Relative Gibbs free energies on different stable spin states are marked with different colors in the diagram.

phosphorene could have a good HER activity with ΔG_{H^*} value of − 0.296 comparable to that of Pt metal, followed by Cu-doped phosphorene with free-energy of − 0.478 eV. Ni-doped phosphorene is also predicted to show a reasonable HER performance with ΔG_{H^*} value of 0.954 eV. ΔG_{H^*} for Ti@phosphorene is much lower than other TMs in the first series, suggesting that the Ti site is the real active site on the phosphorene sheet. It is found that the HER activity of the first transition series doesn't follow any particular trend. Our investigation revealed that Ti, Cu, and Ni-doped phosphorene sheets performed better HER catalytic activity than other transition metals on the first transition series, with Gibbs free energy −0.296, −0.478, and 0.954 eV, respectively. Thus, those metals could be an effective electrocatalyst for hydrogen evolution reaction due to their much low cost and greater availability than expensive noble metals. A graphical representation of the ΔG_{H^*} values of all the transition metals of the first series are given in Fig. 3.

4. Conclusion

First-row TMs have been adsorbed at the phosphorene sheet followed by their optimization at various spin states. Hydrogen is adsorbed on the complex with the most stable spin state to calculate the Gibbs-free energy change (ΔG_{H^*}), which is the key parameter to evaluate the HER catalytic activity for any material. Our results show that Ti@phosphorene ($\Delta G_{H^*} = -0.296$ eV) can be an effective HER electrocatalyst to noble metals if further explored. The value of ΔG_{H^*} calculated for Cu and Ni complexes also exhibits better catalytic activity for HER than the rest of the first transition series metals. These results are also supported by NBO analysis, which demonstrates that the optimum binding of adsorbed intermediate with catalyst surface, in the case of Ti complex, is due to its charge donation ability. Hence, according to the Sabatier principle, the HER catalytic activity for various TM@P is slightly less than state-of-the-art Pt metal. However, a huge cost difference between precious Pt metal and cost-efficient Ni could make it a suitable electrocatalyst for hydrogen production.

Declaration of Competing Interest

The authors declare that they have no known competing financial interests or personal relationships that could have appeared to influence the work reported in this paper.

Data availability

Data will be made available on request.

References

[1] Z. Ge, et al., A Review of the Electrocatalysts on Hydrogen Evolution Reaction With an Emphasis on Fe, Co and Ni-based Phosphides, J. Mater. Sci. 55 (29) (2020) 14081–14104.
[2] I. Dincer, C. Acar, Review and evaluation of hydrogen production methods for better sustainability, Int. J. Hydrogen Energy 40 (34) (2015) 11094–11111.
[3] D.K. Seo, et al., Study of coal pyrolysis by thermo-gravimetric analysis (TGA) and concentration measurements of the evolved species, J. Anal. Appl. Pyrol. 92 (1) (2011) 209–216.
[4] S.A. El-Sayed, M. Mostafa, Pyrolysis characteristics and kinetic parameters determination of biomass fuel powders by differential thermal gravimetric analysis (TGA/DTG), Energy Convers. Manage. 85 (2014) 165–172.
[5] T. Robinson, et al., Sample preparation for thermo-gravimetric determination and thermo-gravimetric characterization of refuse derived fuel, Waste Manag. 48 (2016) 265–274.
[6] E. Goodger, Comparative energies of alternative fuels, Appl. Energy 4 (1) (1978) 39–50.
[7] L. Zhang, et al., Electrochemical Water Electrolysis: Fundamentals and Technologies. 2020: CRC Press.
[8] A. Abánades, C. Rubbia, D. Salmieri, Thermal cracking of methane into hydrogen for a CO_2-free utilization of natural gas, Int. J. Hydrogen Energy 38 (20) (2013) 8491–8496.
[9] N. Dubouis, A. Grimaud, The hydrogen evolution reaction: from material to interfacial descriptors, Chem. Sci. 10 (40) (2019) 9165–9181.
[10] A. Kumar, et al., Direct electrosynthesis of sodium hydroxide and hydrochloric acid from brine streams, Nat. Catal. 2 (2) (2019) 106–113.
[11] J.M. Bockris, E.J.J.o.T.E.S. Potter, The mechanism of the cathodic hydrogen evolution reaction, J. Electrochem. Soc., 1952. **99**(4): p. 169.
[12] S.J. Gutić, et al., Hydrogen Evolution Reaction-From Single Crystal to Single Atom Catalysts, Catalysts 10 (3) (2020) 290.
[13] T. Shinagawa, A.T. Garcia-Esparza, K. Takanabe, Insight on Tafel slopes from a microkinetic analysis of aqueous electrocatalysis for energy conversion, Sci. Rep. 5 (1) (2015) 13801.
[14] H. Gasteiger, et al., Beginning-of-life MEA performance—efficiency loss contributions. Handbook of, Fuel Cells (2010).
[15] Y. Zheng, et al., Advancing the electrochemistry of the hydrogen-evolution reaction through combining experiment and theory, Angew. Chem. Int. Ed. 54 (1) (2015) 52–65.
[16] B. Conway, B. Tilak, Interfacial processes involving electrocatalytic evolution and oxidation of H_2, and the role of chemisorbed H, Electrochim. Acta 47 (22–23) (2002) 3571–3594.
[17] M. Fang, et al., Hierarchical Nanostructures: Hierarchical Nanostructures: Design for Sustainable Water Splitting (Adv. Energy Mater. 23/2017). Advanced Energy Materials, 207(23): p. 1770135.
[18] S.T. Oyama, Novel catalysts for advanced hydroprocessing: transition metal phosphides, J. Catal. 216 (1–2) (2003) 343–352.
[19] V. Zuzaniuk, R. Prins, Synthesis and characterization of silica-supported transition-metal phosphides as HDN catalysts, J. Catal. 219 (1) (2003) 85–96.
[20] S.J. Sawhill, et al., Thiophene hydrodesulfurization over nickel phosphide catalysts: effect of the precursor composition and support, J. Catal. 231 (2) (2005) 300–313.
[21] S.-S. Yi, et al., Noble-metal-free cobalt phosphide modified carbon nitride: an efficient photocatalyst for hydrogen generation, Appl Catal B: Environ. 200 (2017) 477–483.
[22] B. Ma, et al., 5 nm NiCoP nanoparticles coupled with gC_3N_4 as high-performance photocatalyst for hydrogen evolution, Sci. China Mater. 63 (2) (2020) 258–266.
[23] A. Parra-Puerto, et al., Supported transition metal phosphides: activity survey for HER, ORR, OER, and corrosion resistance in acid and alkaline electrolytes, ACS Catal. 9 (12) (2019) 11515–11529.
[24] K. Hu, et al., Iron phosphide/N, P-doped carbon nanosheets as highly efficient electrocatalysts for oxygen reduction reaction over the whole pH range, Electrochim. Acta 254 (2017) 280–286.
[25] S. Sultan, et al., Single Atoms and Clusters Based Nanomaterials for Hydrogen Evolution, Oxygen Evolution Reactions, and Full Water Splitting, 9(22) (2019) p. 1900624.
[26] D. Ma, et al., Computational Evaluation of Electrocatalytic Nitrogen Reduction on TM Single-, Double-, and Triple-Atom Catalysts (TM = Mn, Fe Co, Ni) Based on Graphdiyne Monolayers, J. Phys. Chem. C 123 (31) (2019) 19066–19076.
[27] J.N. Tiwari, et al., Recent Advancement of p- and d-Block Elements, Single Atoms, and Graphene-Based Photoelectrochemical Electrodes for Water Splitting, 10(24) (2020) p. 2000280.
[28] J.N. Tiwari, et al., Multicomponent electrocatalyst with ultralow Pt loading and high hydrogen evolution activity, 3(9) (2018) p. 773-782.
[29] S. Sultan, et al., Modulation of Cu and Rh single-atoms and nanoparticles for high-performance hydrogen evolution activity in acidic media, 9(16) (2021) p. 10326-10334.
[30] Y. Wang, et al., Enabling multifunctional electrocatalysts by modifying the basal plane of unifunctional 1T′-MoS 2 with anchored transition metal single atoms, 13 (31) (2021) p. 13390-13400.

[31] Y. Wang, et al., Theoretical insights into the electroreduction of nitrate to ammonia on graphene-based single-atom catalysts, 14(30) (2022) p. 10862-10872.
[32] D. Wu, et al., Double-atom catalysts for energy-related electrocatalysis applications: a theoretical perspective, 2022.
[33] M. Ha, et al., Tuning metal single atoms embedded in NxCy moieties toward high-performance electrocatalysis, Energ. Environ. Sci. 14 (6) (2021) 3455–3468.
[34] P. Liu, J.A. Rodriguez, Catalysts for hydrogen evolution from the [NiFe] hydrogenase to the Ni_2P (001) surface: the importance of ensemble effect, J. Am. Chem. Soc. 127 (42) (2005) 14871–14878.
[35] Y. Xu, et al., Anion-exchange synthesis of nanoporous FeP nanosheets as electrocatalysts for hydrogen evolution reaction, Chem. Commun. 49 (59) (2013) 6656–6658.
[36] H. Du, et al., Template-Assisted Synthesis of CoP Nanotubes to Efficiently Catalyze Hydrogen-Evolving Reaction, J. Mater. Chem. A 2 (36) (2014) 14812–14816.
[37] J.M. McEnaney, et al., Electrocatalytic hydrogen evolution using amorphous tungsten phosphide nanoparticles, Chem. Commun. 50 (75) (2014) 11026–11028.
[38] Z. Pu, et al., Tungsten phosphide nanorod arrays directly grown on carbon cloth: a highly efficient and stable hydrogen evolution cathode at all pH values, ACS Appl. Mater. Interfaces 6 (24) (2014) 21874–21879.
[39] J.M. McEnaney, et al., Amorphous molybdenum phosphide nanoparticles for electrocatalytic hydrogen evolution, Chem. Mater. 26 (16) (2014) 4826–4831.
[40] P. Xiao, et al., Molybdenum phosphide as an efficient electrocatalyst for the hydrogen evolution reaction, Energy Environ. Sci. 7 (8) (2014) 2624–2629.
[41] J. Tian, et al., Self-supported Cu_3P nanowire arrays as an integrated high-performance three-dimensional cathode for generating hydrogen from water, Angew. Chem. 126 (36) (2014) 9731–9735.
[42] A. Han, et al., Crystalline copper phosphide nanosheets as an efficient janus catalyst for overall water splitting, ACS Appl. Mater. Interfaces 9 (3) (2017) 2240–2248.
[43] Z. Sofer, et al., Back Cover: Layered Black Phosphorus: Strongly Anisotropic Magnetic, Electronic, and Electron-Transfer Properties (Angew. Chem. Int. Ed. 10/2016), Angewandte Chem. Int. Ed. 55(10) (2016) p. 3516-3516.
[44] F.F. Schweinberger, et al., Cluster size effects in the photocatalytic hydrogen evolution reaction, J. Am. Chem. Soc. 135 (36) (2013) 13262–13265.
[45] S. Yu, et al., C_2N: an excellent catalyst for the hydrogen evolution reaction, Phys. Chem. Chem. Phys. 20 (44) (2018) 27970–27974.
[46] S.T. Thompson, D. Papageorgopoulos, Platinum group metal-free catalysts boost cost competitiveness of fuel cell vehicles, Nat. Catal. 2 (7) (2019) 558–561.
[47] G. Gao, Q. Sun, A. Du, Activating catalytic inert basal plane of molybdenum disulfide to optimize hydrogen evolution activity via defect doping and strain engineering, J. Phys. Chem. C 120 (30) (2016) 16761–16766.
[48] C. Wan, Y.N. Regmi, B.M. Leonard, Multiple phases of molybdenum carbide as electrocatalysts for the hydrogen evolution reaction, Angew. Chem. 126 (25) (2014) 6525–6528.
[49] X. Zhou, et al., Symmetrical synergy of hybrid Co_9S_8-MoS_x electrocatalysts for hydrogen evolution reaction, Nano Energy 32 (2017) 470–478.
[50] D.J. Li, et al., Molybdenum Sulfide/N-Doped CNT Forest Hybrid Catalysts for High-Performance Hydrogen Evolution Reaction, Nano Lett. 14 (3) (2014) 1228–1233.
[51] R. Anand, et al., Late Transition Metal Doped MXenes Showing Superb Bifunctional Electrocatalytic Activities for Water Splitting via Distinctive Mechanistic Pathways, Adv. Energy Mater. 11 (48) (2021) 2102388.
[52] M. Umer, et al., Machine learning assisted high-throughput screening of transition metal single atom based superb hydrogen evolution electrocatalysts, J. Mater. Chem. A 10 (12) (2022) 6679–6689.
[53] P. Xiao, et al., Novel molybdenum carbide–tungsten carbide composite nanowires and their electrochemical activation for efficient and stable hydrogen evolution, Adv. Funct. Mater. 25 (10) (2015) 1520–1526.
[54] D. Voiry, et al., Conducting MoS_2 nanosheets as catalysts for hydrogen evolution reaction, Nano Lett. 13 (12) (2013) 6222–6227.
[55] Q. Jiang, et al., Facile synthesis of black phosphorus: an efficient electrocatalyst for the oxygen evolving reaction, Angew. Chem. 128 (44) (2016) 14053–14057.
[56] X. Ren, et al., Few-layer black phosphorus nanosheets as electrocatalysts for highly efficient oxygen evolution reaction, Adv. Energy Mater. 7 (19) (2017) 1700396.
[57] L. Shao, et al., Facile preparation of NH_2-functionalized black phosphorene for the electrocatalytic hydrogen evolution reaction, J. Mater. Chem. A 6 (6) (2018) 2494–2499.
[58] C.C. Mayorga-Martinez, et al., Black Phosphorus Nanoparticle Labels for Immunoassays via Hydrogen Evolution Reaction Mediation, Anal. Chem. 88 (20) (2016) 10074–10079.
[59] R. He, et al., Molybdenum Disulfide-Black Phosphorus Hybrid Nanosheets as a Superior Catalyst for Electrochemical Hydrogen Evolution, Nano Lett. 17 (7) (2017) 4311–4316.
[60] Y. Gan, et al., Chemically modified phosphorene as efficient catalyst for hydrogen evolution reaction, J. Phys. Condens. Matter 32 (2) (2019), 025202.
[61] J.N. Tiwari, et al., Multi-heteroatom-doped carbon from waste-yeast biomass for sustained water splitting, Nat. Sustain. 3 (7) (2020) 556–563.
[62] H. Jin, et al., Simple and Scalable Mechanochemical Synthesis of Noble Metal Catalysts with Single Atoms toward Highly Efficient Hydrogen Evolution, Adv. Funct. Mater. 30 (25) (2020) 2000531.
[63] A.M. Harzandi, et al., Immiscible bi-metal single-atoms driven synthesis of electrocatalysts having superb mass-activity and durability, Appl Catal B: Environ. 270 (2020), 118896.
[64] N.K. Dang, et al., Surface enrichment of iridium on IrCo alloys for boosting hydrogen production, J. Mater. Chem. A 9 (31) (2021) 16898–16905.
[65] Y. Zheng, et al., Hydrogen evolution by a metal-free electrocatalyst, Nat. Commun. 5 (1) (2014) 1–8.
[66] J.P. Perdew, K. Burke, M. Ernzerhof, Generalized gradient approximation made simple, Phys. Rev. Lett. 77 (18) (1996) 3865.
[67] J. Perdew, J.P. Perdew, K. Burke, M. Ernzerhof, Phys. Rev. Lett. 78 (1997) p. 1396.
[68] M. Frisch, et al., Gaussian Inc, Wallingford CT, 2013. **1**.
[69] F. Weigend, R. Ahlrichs, Balanced basis sets of split valence, triple zeta valence and quadruple zeta valence quality for H to Rn: Design and assessment of accuracy, Phys. Chem. Chem. Phys. 7 (18) (2005) 3297–3305.
[70] S. Grimme, Chem., 2004, 25, 1463; S. Grimme, J. Antony, S. Ehrlich and H. Krieg. J. Chem. Phys, 2010. **132**: p. 154104.
[71] S. Grimme, S. Ehrlich, L. Goerigk, Effect of the damping function in dispersion corrected density functional theory, J. Comput. Chem. 32 (7) (2011) 1456–1465.
[72] P. Sabatier, La catalyse en chimie organique, Paris et Liege: Librairie polytechnique, 1920.
[73] X. Liu, et al., A computational study on Pt and Ru dimers supported on graphene for the hydrogen evolution reaction: new insight into the alkaline mechanism, J. Mater. Chem. A 7 (8) (2019) 3648–3654.
[74] J. Greeley, et al., Computational high-throughput screening of electrocatalytic materials for hydrogen evolution, Nat. Mater. 5 (11) (2006) 909–913.
[75] B.H. Solis, S. Hammes-Schiffer, Computational Study of Anomalous Reduction Potentials for Hydrogen Evolution Catalyzed by Cobalt Dithiolene Complexes, J. Am. Chem. Soc. 134 (37) (2012) 15253–15256.
[76] A. Bhattacharjee, et al., A Computational Study of the Mechanism of Hydrogen Evolution by Cobalt(Diimine-Dioxime) Catalysts, A Eur. J. 19 (45) (2013) 15166–15174.
[77] M. Gomez-Mingot, et al., Bioinspired Tungsten Dithiolene Catalysts for Hydrogen Evolution: A Combined Electrochemical, Photochemical, and Computational Study, J. Phys. Chem. B 119 (43) (2015) 13524–13533.
[78] G. Hu, Q. Tang, D.-E. Jiang, CoP for hydrogen evolution: implications from hydrogen adsorption, Phys. Chem. Chem. Phys. 18 (34) (2016) 23864–23871.
[79] J.K. Nørskov, et al., Trends in the exchange current for hydrogen evolution, J. Electrochem. Soc. 152 (3) (2005) J23.
[80] M.H. Butt, et al., Cu-doped phosphorene as highly efficient single atom catalyst for CO oxidation: A DFT study, Mol. Catal. 509 (2021), 111630.
[81] H. Liu, et al., Phosphorene: an unexplored 2D semiconductor with a high hole mobility, ACS Nano 8 (4) (2014) 4033–4041.
[82] J. Lim, et al., Ultralow Overpotential of Hydrogen Evolution Reaction using Fe-Doped Defective Graphene: A Density Functional Study, ChemCatChem 10 (19) (2018) 4450–4455.
[84] V. Perazzolo, et al., Density Functional Theory (DFT) and Experimental Evidences of Metal-Support Interaction in Platinum Nanoparticles Supported on Nitrogen- and Sulfur-Doped Mesoporous Carbons: Synthesis, Activity, and Stability, ACS Catal. 8 (2) (2018) 1122–1137.
[85] C. Liu, et al., Conversion of dinitrogen to ammonia on Ru atoms supported on boron sheets: a DFT study, 7(9) (2019) p. 4771-4776.
[86] C. Ling, et al., Nanosheet supported single-metal atom bifunctional catalyst for overall water splitting, 17(8) (2017) p. 5133-5139.
[87] G. Vilé, et al., A stable single-site palladium catalyst for hydrogenations, 54(38) (2015) p. 11265-11269.
[88] G. Gao, et al., Single atom (Pd/Pt) supported on graphitic carbon nitride as an efficient photocatalyst for visible-light reduction of carbon dioxide, 138(19) (2016) 6292–6297.
[89] I. Jang, et al., Electron-deficient titanium single-atom electrocatalyst for stable and efficient hydrogen production, Nano Energy 78 (2020), 105151.
[90] J. Zhu, et al., Recent advances in electrocatalytic hydrogen evolution using nanoparticles. 120(2) (2019) p. 851-918.